Minimum energy dissipation river networks with fractal boundaries

Tao Sun, Paul Meakin, and Torstein Jøssang
Department of Physics, University of Oslo, P.O. Box 1048 Blindern, 0316 Oslo, Norway
and Center for Advanced Study at The Norwegian Academy of Science and Letter, P.O. Box 7606 Skillebekk, 0205 Oslo, Norway
(Received 31 October 1994; revised manuscript received 23 January 1995)

The effects of the entire drainage area boundary on the drainage basins and their size distributions have been studied using the minimum energy dissipation model for river networks. A simple scaling relationship $\tau=1+D/2$ between the values of the exponents τ in the power law basin size distibutions and the fractal dimension D of the boundary of the entire drainage area has been established. The scaling relationship has been tested using simulations, with external perimeters ($D=\frac{4}{3}$) or hulls ($D=\frac{7}{4}$) of invasion percolation clusters, as the boundaries for the entire drainage areas.

PACS number(s): 64.60.Ht, 92.40.Fb, 92.40.Cy, 02.60.Pn

Drainage networks that are embedded in a drainage area subject to a uniform energy input from precipitation have frequently been cited as familiar examples of a spatially extended open system [1]. Precipitated water flows downhill, through channel networks, and finally ends its journey in an ocean or lake. During this process, the potential energy associated with the precipitation is dissipated. Drainage area landscapes are modified by erosion caused by the flow, and self-organize into structures that have often been described as self-similar fractals [2–6]. The whole drainage area is partitioned into a number of drainage basins and their boundaries are found to be fractal [7]. The distributions of a number of physical variables in river basins are multifractal [8]. These physical variables include energy expenditure, slopes, and discharge. It has also been argued that the evolution of drainage networks displays multiscaling properties [9] and spatial self-organized criticity [10–13].

A number of models for drainage networks have been developed in order to understand these spatially extended open systems. All these models can be approximately separated into three classes according to their different approaches. The models in the first class are based on Shreve's fundamental stochastic postulate of random topology [14–17]. The second type is mainly based on optimization principles [18–21]. These models embody the assumption that an open system with constant energy injections tends to form a structure that minimizes the total energy dissipation rate in the system [22,23]. Both the first and the second types of models have focused on reproducing the statistical properties of drainage networks while less emphasis has been placed on their evolution. Unlike the first two types of models, the third class of models [6,24–27] is based on physical processes, such as erosion and deposition, which alter the landscape of the drainage area that dictates the configurations of river networks.

Recently, models of the second type, described above, have been studied extensively by Howard [21] and Rinaldo *et al.* [28]. The model of Rinaldo *et al.* is based on three principles of optimal energy expenditure proposed by Rodriguez-Iturbe *et al.* [29]: (1) the principle of minimum energy expenditure in any link of the network, (2) the principle of equal energy expenditure per unit area of channel surface anywhere in the network, and (3) the principle of minimum energy expenditure in the network as a whole. Provided with the position of an outlet and the outer basin boundary, the structure of the minimum energy dissipation river network that drains the given basin is obtained. The structural characteristics of the minimum energy dissipation drainage network, such as Horton's law of stream lengths, the stream's bifurcation ratio, and the multifractal spectrum of the width function, are found to be similar to those measured for natural drainage networks [30]. The model of Rinaldo *et al.* has been extended to the case in which the drainage area can be covered by a number of river basins [31]. The boundary of each basin is determined, in a natural way, by the competition (minimizing the energy dissipation rate in the network) and cooperation (covering of the whole drainage area) between the basins that share common boundaries. It had been found that the distribution of drainage basin areas obtained from this model is a power law. The boundary of each drainage basin is also a fractal with a fractal dimension of about 1.10 and the structure of the minimum energy dissipation river networks are self-similar in terms of the scaling relationship between the internal link length distribution and the network resolution. These results are also similar to the field data obtained from studies of natural drainage basins [31].

A minimum energy dissipation model [32], based on that of Howard [20] and Rinaldo *et al.* [28], is based directly on the minimum energy dissipation principle and an empirical relationship [33] $s\sim Q^{\alpha}$ between the slope s of each link in a channel network and the mean annual discharge Q that flows through it. Field observations indicate that the velocity of water flow is almost constant everywhere in a channel network [34]. The constant velocity of water flow and the small magnitude of the velocity everywhere means that the contribution of changes in kinetic energy to the energy dissipation in the stream is negligible. If P_i denotes the energy dissipation in link i of length L_i, Q_i is the mean discharge in link i, and s_i is the

slope in that link, then the energy dissipation in the link can be written as

$$P_i = Q_i L_i s_i = Q_i^{1+\alpha} L_i \ . \quad (1)$$

Here the relationship

$$s_i \sim Q_i^{\alpha} \quad (2)$$

has been applied. Thus the total energy dissipation in the whole drainage network can be expressed as

$$P = \sum_i P_i = \sum_i Q_i^{1+\alpha} L_i \ , \quad (3)$$

where the index i sums over all the links. The landscape is associated with the drainage network by

$$h_i = \sum_j s_j L_j = \sum_j Q_j^{\alpha} L_j \ . \quad (4)$$

Here h_i is the elevation of site i on the landscape and the index j labels all of the links connecting site i to the outlet on the boundary of A, where the height is 0 (sea level). The flow Q_i is calculated as

$$Q_i = \sum_j Q_j + 1 \ , \quad (5)$$

where it is assumed that precipitation falls uniformly on the whole the area A and there are no losses due to evaporation, subsurface flow, etc. The summation is over all the tributaries j of i that have flows of Q_j into site i. The addition of a unit flow to $\sum_j Q_j$ represents the precipitation onto the ith site.

The value of α is given by Leopold and Maddock [33] as -0.49. However, a large range of values has been obtained for the exponent α from field observations [34–37]. The value of α can also be derived theoretically, based on the three optimal energy expenditure principles for channel networks [29]. This theoretical value is -0.5. So when a value of -0.5 is used for α, this model is identical to that of Rinaldo *et al.*

The model was studied [32] using six different values for the exponent α ($\alpha = -0.75$, -0.625, -0.5, -0.325, -0.25, and -0.125). The surfaces of these minimum energy dissipation drainage basins were constructed and found to be more complex than simple self-affine fractals. The drainage basins of these optimal drainage networks have power law size (area) distribution $N(A) \sim A^{-\tau}$ with a universal exponent $\tau = \frac{3}{2}$ which is independent of the value of α. For the minimum energy dissipation drainage networks, obtained using a particular value for α, the basins shape are similar to each other.

To a significant degree, all three types of models, discussed above, have reproduced the geometrical and topological proprieties that characterize natural drainage basins, especially their scaling (fractal) properties [6,17,29–32]. In minimum energy dissipation models [29–32], the structure of drainage networks and their associated landscapes, which recreate many scaling properties that are also found in nature, were obtained as the coproducts of the minimum energy dissipation principle and space filling. The space is defined by the outer boundary of the drainage area. In all the previous studies, the lattice boundary (a square) was used as the boundary for the whole drainage area. Few studies have addressed the roll of this boundary in the organization of the river basins.

Here, a more realistic, fractal boundary has been used for the entire system in the model. The implementation of the model and the optimization method have been described earlier [32].

Two types of fractal boundaries were used for the entire drainage area. They are the external perimeters and the hulls of invasion percolation clusters [38–42]. Figure 1(a) shows the area enclosed by the external perimeter of an invasion percolation cluster, generated on a square lattice. The entire area enclosed by these fractal boundaries (including both invaded and trapped regions) is used as the area A in the simulations. The maximum extent of the invasion percolation cluster is 256 lattice units so that the whole cluster can be embedded in a 256×256 triangular lattice. When the hull of an invasion percolation cluster is used for the boundary of the entire drainage area, those unoccupied areas, which can be connected from outside the region occupied by the cluster through a path consisting of steps between either unoccupied nearest neighbors or unoccupied next nearest neighbors, were excluded [42]. It has been shown [40–45] that the fractal dimensions for the external perimeter and the hull of a percolation cluster, or a cluster obtained by invasion percolation growth without trapping rules, are exactly $\frac{4}{3}$ and $\frac{7}{4}$. The fractal dimension of the external perimeter of an invasion percolation cluster is not affected by trapping rules. However, it can be shown that the fractal dimension of an invasion percolation cluster grown with trapping rules differs from the value of $\frac{7}{4}$ [46,47]. Figure 1(b) shows an example of a drainage area using the hull of an invasion percolation cluster grown without trapping rules as its boundary. Its maximum extent was 512 lattice units.

Different values of the exponent α and the sizes of the invasion percolation clusters were tested in the simulations. The resulting structures of the individual minimum energy dissipation drainage networks, were all found to be similar to those obtained from the simulations using square boundaries, with corresponding values for the exponent α. Figure 2 shows an example of a minimum energy dissipation drainage network, obtained using the external perimeters of an invasion percolation cluster with maximum extension of 256, and a value of -0.5 for the exponent α.

It can be seen from the figures that the whole drainage area is drained by a distribution of river networks of different sizes. This partition of the drainage area, together with the structures within each river network, minimizes the total energy dissipation rate in the whole system. Figures 3(a) and 3(b) show the boundaries between the river basins in two drainage areas with the external perimeter and the hull of an invasion percolation cluster as their boundaries, respectively. These boundaries define each individual drainage basin inside the en-

tire drainage area. Within each drainage basin, all the water will sooner or later reach the same outlet and flow out of the entire area into the "ocean."

The cumulative size distributions of the drainage basins for different values of α and using different fractal boundaries are shown in Figs. 4(a) and 4(b). All the data sets used in the Fig. 4(a) were obtained using external perimeters of invasion percolation clusters as their entire drainage areas boundaries. The data sets shown in Fig. 4(b) were obtained from simulations carried out using invasion percolation cluster hulls as boundaries for the entire drainage areas. In Fig. 4(a), the data sets represented by the square symbols correspond to the drainage areas with maximum extensions L of 512 lattice units, while for the other data sets $L=256$ lattice units. The values of the exponent α used in the simulations were -0.75, -0.5, and -0.25 corresponding to the data sets represented by the diamond, circle or square, and triangle symbols, respectively. In Fig. 4(b), the maximum extent of the drainage area was 512 lattice units, and the value of the exponent α was -0.5, for all the data sets shown in the figure.

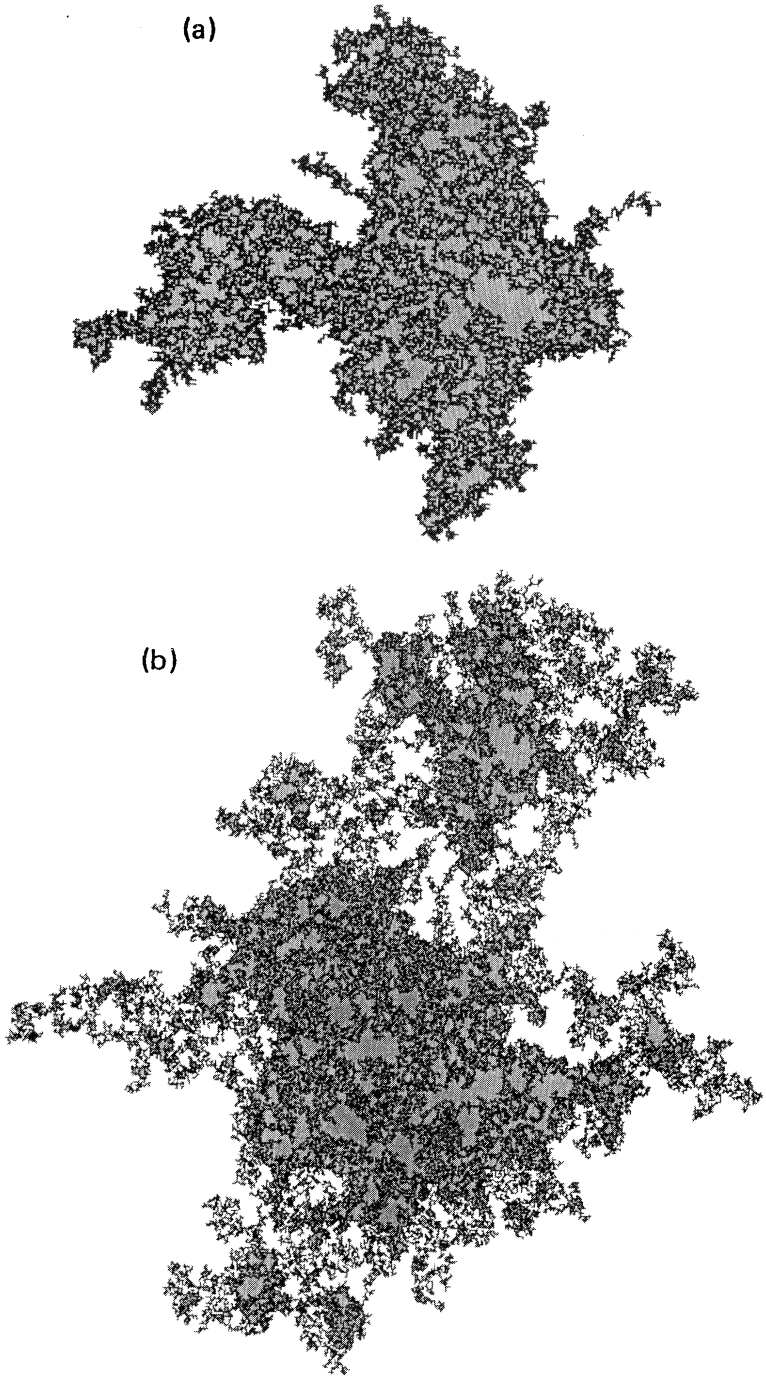

FIG. 1. Examples of two drainage areas used in the simulations. In Fig. 1(a), the boundary of the drainage area is the external perimeter of the invasion percolation cluster. The black sites are invaded sites and the gray sites are trapped sites. The maximum extension ($L=x_{\max}-x_{\min}$) is 256 lattice units. In Fig. 1(b), the boundary of the drainage area is the hull of an invasion percolation cluster. Those trapped areas in the cluster that can be connected to the outside through a path consisting of steps between unoccupied nearest neighbors or unoccupied next nearest neighbors are not included in the drainage area. Trapped regions that cannot be reached in this manner are shown in gray. The cluster extends over a length of 512 lattice units. In both parts of the figure, the entire drainage areas used in the simulations are indicated by the black sites and gray sites.

All the data sets in Figs. 4(a) and 4(b) can be fitted quite well by straight lines over more than a decade of basin areas. This means that the minimum energy dissipation drainage basins in the drainage area with a fractal boundary have a power law cumulative size distribution $N(A > A^*) \sim A^{*1-\tau}$, where the value of $1-\tau$ is given by the slope of these fitted lines. In other words, the basin area distribution is $N(A) \sim A^{-\tau}$, where $N(A)\delta A$ is the number of basins with areas in the range $A-\delta A/2$ to $A+\delta A/2$. The slopes of the fitting straight lines shown in Figs. 4(a) and 4(b) are close to each other. This indicates that the values of the exponent τ are close to each other when the data sets are obtained from simulations using boundaries with the same fractal dimension, independent of the values of the exponent α used in the simulation.

A power law distribution of basin area was also found in previous studies in which a square was used as the boundary for the whole drainage area [32]. However, with square boundaries, a value of -1.50 was found for the size distribution exponent τ. This indicates that the value of τ depends on the fractal dimension of the boundary. The relationship between τ and D can be explained by a scaling argument similar to that used by Meakin, Feder, and Jøssang [17] to explain the power law basin area distribution found using simple statistical models for river networks.

Assuming that the basin area distribution is given by

$$N(A) \sim A^{-\tau} , \tag{6}$$

then the total area $\mathcal{A}$ occupied by basins of area $A < A^*$ is given by

$$\begin{aligned} \mathcal{A} &\sim \int_0^{A^*} A A^{-\tau} dA \\ &\sim [A^{2-\tau}]_0^{A^*} \\ &\sim A^{*2-\tau} . \end{aligned} \tag{7}$$

It has been shown that the basins obtained from the drainage area with particular values of α are similar to each other [32] (their aspect ratio is ≈ 1 and does not increase with increasing basin area). This implies that for each basin, the basin area scales as

$$A^* \sim l^{*2} , \tag{8}$$

where l^* is the length of the basin. Substituting Eq. (8) into Eq. (7), it can be seen that

$$\mathcal{A} \sim l^{*2(2-\tau)} . \tag{9}$$

The area within distance l^* from a D dimensional boundary can approximately by the sum of the areas of the maximum number of boxes with side length l^* that are needed to cover the entire boundary. Thus

$$\mathcal{A} \sim l^{*2} l^{*-D} = l^{*2-D} . \tag{10}$$

Comparing Eqs. (9) and (10), it can be seen that

$$\tau = 1 + D/2 . \tag{11}$$

If a square is used as the whole drainage area, the di-

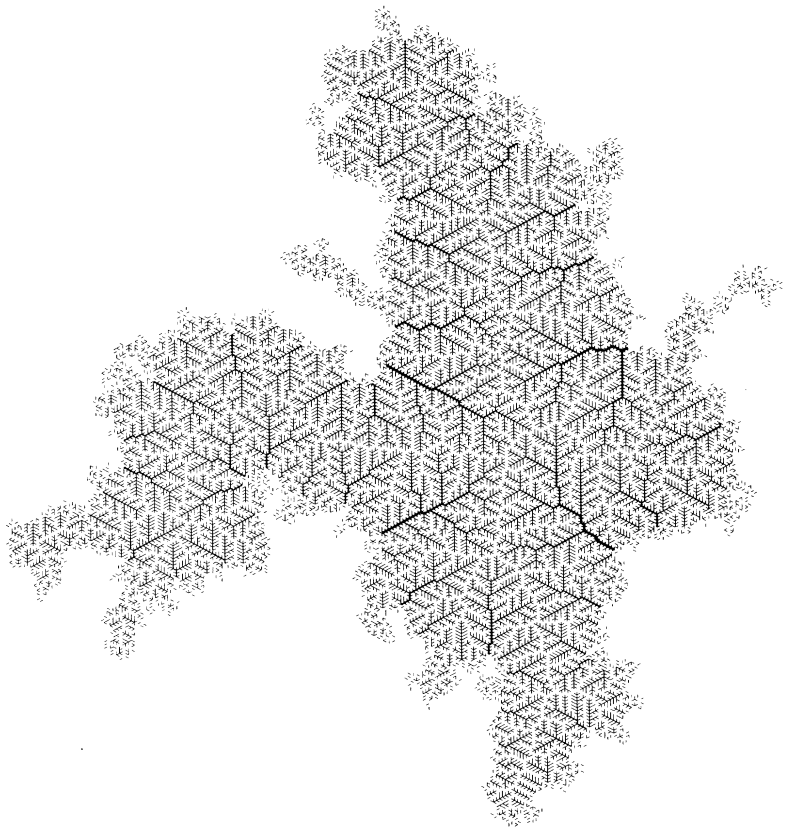

FIG. 2. River networks generated from the minimum energy dissipation model using fractal boundaries. The boundary of the entire drainage area used in the simulation was obtained from the external perimeter of the invasion percolation cluster shown in Fig. 1(a). A value of -0.50 was used for the exponents α in the simulation. The thickness of the links (segments in the figure) is plotted proportional to the square root of the flow in that link. The arrows indicate the flow directions in the networks.

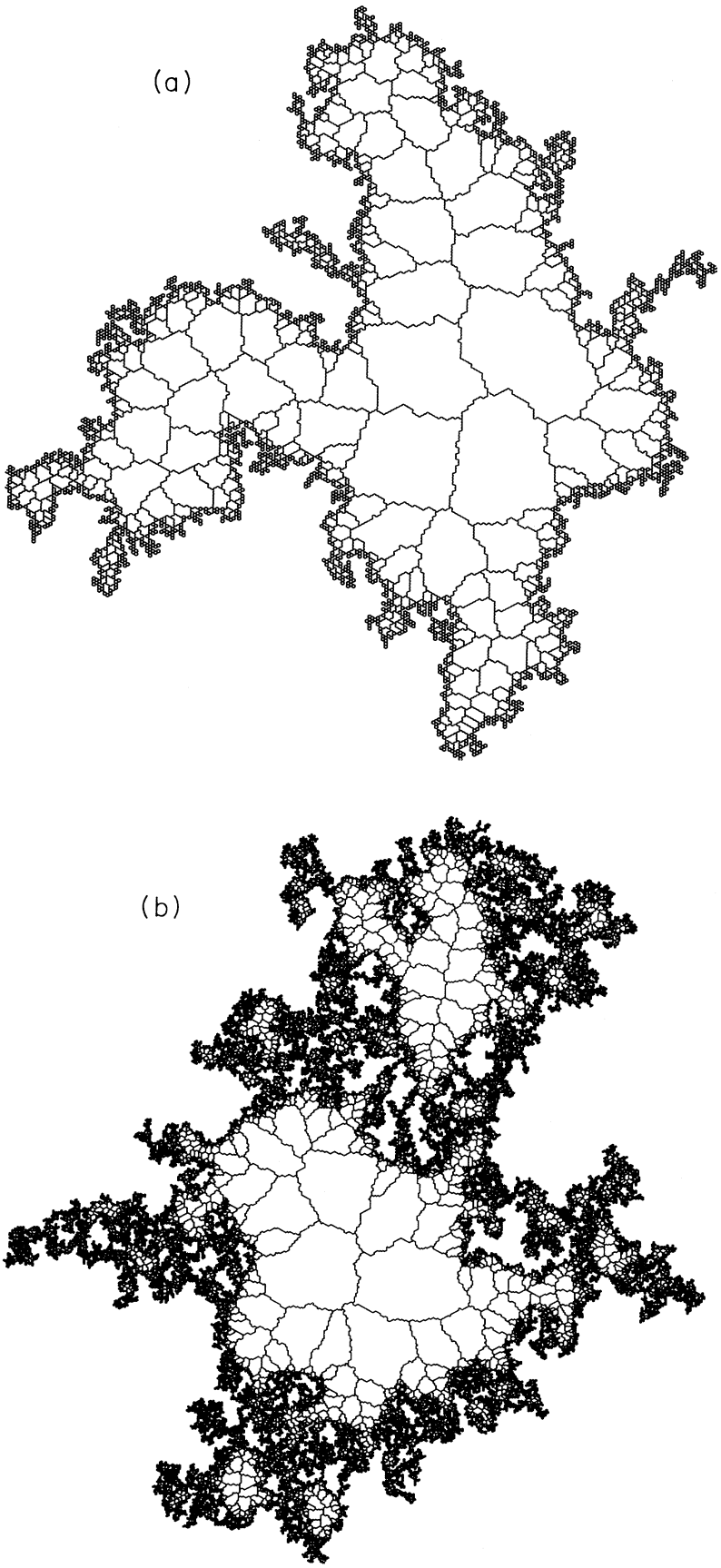

FIG. 3. The boundaries of the minimum energy dissipation drainage basins. The boundaries of the entire drainage area used to generate Figs. 3(a) and 3(b) are shown in Fig. 1(a) and 1(b), respectively. A value of -0.5 was used for the exponent α in both the simulations.

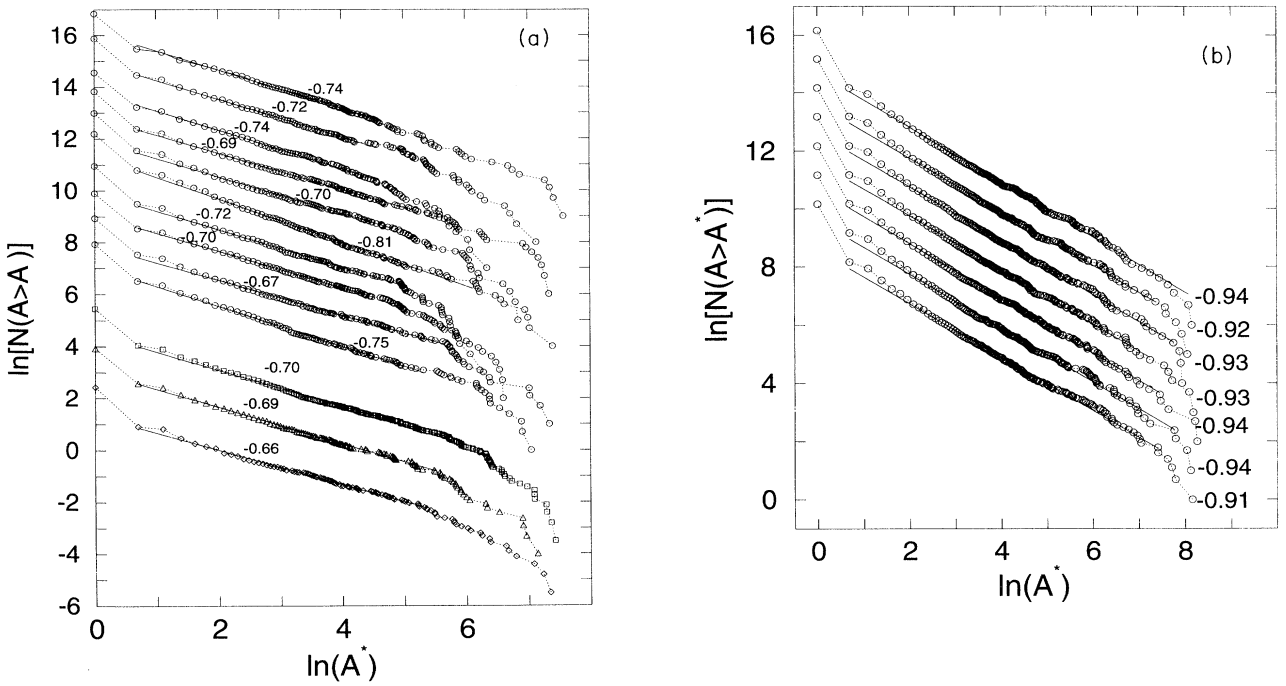

FIG. 4. The dependence of $N(A > A^*)$, the number of the basins that have areas larger than A^*, on the area A^* for different values of α and the two different types of drainage area boundaries. In Fig. 4(a), all the data sets were obtained by using fractal boundaries obtained from invasion percolation cluster external perimeters. Results obtained from simulations carried out with $\alpha=-0.25$, -0.5, and -0.75 are indicated by triangular, square or circular, and diamond shaped symbols, respectively. The maximum extent L of the entire drainage area was 512 lattice units corresponding to the square symbols, while all the other simulations were carried out with $L=256$ lattice units. In Fig. 4(b), the hulls of invasion percolation clusters were used as boundaries. In these simulations $\alpha=-0.5$ and $L=512$. In both parts of the figure, the data sets are fitted by straight lines using a "least-squares-fitting" method. The slopes of these lines are indicated. The data points belonging to the same data set are connected by dotted lines to guide the eye.

mension of the boundary D is 1. According to Eq. (11), the value of τ is $\frac{3}{2}$. This is the result that was obtained in the earlier studies. For the simulations with invasion percolation cluster external perimeter boundaries with a fractal dimension $D=\frac{4}{3}$, a value of $\tau=\frac{5}{3}$ is expected from the scaling exponent relationship between τ and D in Eq. (11). The values of τ obtained from the simulations are 1.66, 1.69, 1.70, 1.75, 1.67, 1.70, 1.72, 1.81, 1.70, 1.69, 1.74, 1.72, and 1.74, with a mean value of 1.71. All of these values are close to the theoretical value of 1.67. When the entire drainage area boundaries were obtained from the hull of invasion percolation clusters with a fractal dimension of $\frac{7}{4}$, a value of the $\tau=\frac{15}{8}=1.875$ is expected. The values of τ, obtained from the data sets shown in Fig. 4(b), are 1.94, 1.92, 1.93, 1.93, 1.94, 1.94, and 1.91, with a mean value of 1.93. These values are also close to the theoretical value of 1.875. This suggests that the minimum energy dissipation drainage basins have a power law basin area distribution $N(A)\sim A^{-\tau}$, with a value of $1+D/2$ for the exponent τ, where D is the fractal dimension of the boundary of the entire drainage area that encloses all the drainage basins. For drainage areas with boundaries that have the same fractal dimensions, the number of basins with size A in the drainage area appears to decay algebraically with the same universal exponent for different values of α.

The other quantities that characterize drainage basins, such as the fractal dimension of individual basin perimeters, the fractal dimension of main streams, the roughness of the resulting landscape and the fractal dimension of its contours, etc., have also been investigated. These quantities were found to be independent of the fractal dimension of the entire drainage basin boundary.

In this paper, the minimum energy dissipation model for river networks has been used to investigate the effects of the entire drainage area boundaries on a number of quantities that characterize drainage basins. Although the studies are restricted to the minimum energy dissipation model, the results may be relevant to the other river network models in which the basin area A is proportional to the square of its length l. If basins of different sizes are related by a more general affine transformation ($A\sim l^{1/\nu_\parallel}$), then the size distribution exponent τ is given by $\tau=2-\nu_\parallel(2-D)$.

We would like to thank G. Wagner for providing his programs to generate the invasion percolation clusters used in the paper.

[1] H. Takayasu, I. Nishikawa, and H. Tasaki, Phys. Rev. A **37**, 3110 (1988).
[2] D. G. Tarboton, R. L. Bras, and I. Rodriguez-Iturbe, Water Res. Res. **24**, 1317 (1988).
[3] P. L. Barbera and R. Rosso, Water Res. Res. **25**, 735 (1989).
[4] A. Robert and A. G. Roy, Water Res. Res. **26**, 839 (1990).
[5] R. Rosso, B. Bacchi, and P. L. Barbera, Water Res. Res. **27**, 381 (1991).
[6] H. Inaoka and H. Takayasu, Phys. Rev. E **47**, 899 (1993).
[7] S. P. Breyer and R. S. Snow, Geomorphology **5**, 143 (1992).
[8] E. J. Ijjasz-Vasquez, I. Rodriguez-Iturbe, and R. L. Bras, Geomorphology **5**, 297 (1992).
[9] D. G. Tarboton, R. L. Bras, and I. Rodriguez-Iturbe, Water Res. Res. **25**, 2037 (1989).
[10] P. Bak, C. Tang, and K. Weisenfeld, Phys. Rev. A **38**, 364 (1988).
[11] H. Takayasu and H. Inaoka, Phys. Rev. Lett. **68**, 966 (1992).
[12] A. Rinaldo, I. Rodriguez-Iturbe, R. Rigon, E. Ijjasz-Vasquez, and R. L. Bras, Phys. Rev. Lett. **70**, 822 (1993).
[13] R. Rigon, A. Rinaldo, and I. Rodriguez-Iturbe, J. Geophys. (to be published).
[14] R. L. Shreve, J. Geol. **74**, 17 (1966).
[15] R. L. Shreve, J. Geol. **75**, 178 (1967).
[16] C. P. Stark, Nature **352**, 423 (1991).
[17] P. Meakin, J. Feder, and T. Jøssang, Physica A **176**, 409 (1991).
[18] R. E. Horton, EOS Trans. AGU **13**, 350 (1932).
[19] L. B. Leopold and W. B. Langbein, U.S. Geol. Surv. Prof. Paper **500A**, 1 (1962).
[20] A. D. Howard, Water Res. Res. **7**, 863 (1971).
[21] A.D. Howard, Water Res. Res. **26**, 2107 (1990).
[22] P. S. Stevens, *Patterns in Nature* (Little, Brown, Boston, 1974).
[23] I. Prigogine, *From Being to Becoming—Time and Complexity in the Physical Sciences* (Freeman, San Francisco, 1980).
[24] P. Meakin, Rev. Geophys. **29**, 317 (1991).
[25] G. Willgoose, R. L. Bras, and I. Rodriguez-Iturbe, Water Res. Res. **27**, 1671 (1991).
Res. Res. **27**, 1671 (1991).
[26] S. Kramer and M. Marder, Phys. Rev. Lett. **68**, 205 (1992).
[27] R. L. Leheny and S. R. Nagel, Phys. Rev. Lett. **71**, 1470 (1993).
[28] A. Rinaldo, I. Rodriguez-Iturbe, R. Rigon, R. L. Bras, E. Ijjasz-Vasquez, and A. Marani, Water. Res. Res. **28**, 2183 (1992).
[29] I. Rodriguez-Iturbe, A. Rinaldo, R. Rigon, R. L. Bras, A. Marani, and E. Ijjasz-Vasquez, Water Res. Res. **28**, 1095 (1992).
[30] I. Rodriguez-Iturbe, A. Rinaldo, R. Rigon, R. L. Bras, E. Ijjasz-Vasquez, and A. Marani, Geophys. Res. Lett. **19**, 889 (1992).
[31] T. Sun, P. Meakin, and T. Jøssang, Phys. Rev. E **49**, 4865 (1994).
[32] T. Sun, P. Meakin, and T. Jøssang, Water Res. Res. **30**, 2599 (1994).
[33] L. B. Leopold and T. Maddock, Jr., U. S. Geol. Surv. Prof. Paper **252**, 56 (1953).
[34] L. B. Leopold, Am. J. Sci. **251**, 606 (1953).
[35] M. G. Wolman, U. S. Geol. Surv. Prof. Paper **272**, 56 (1955).
[36] L. B. Leopold and J. P. Miller, U. S. Geol. Surv. Prof. Paper **282-A**, (1956).
[37] J. J. Flint, Water Res. Res. **10**, 969 (1974).
[38] R. Chandler, J. Koplik, K. Lerman, and J. F. Willemsen, J. Fluid Mech. **119**, 249 (1982).
[39] D. Wilkinson and J. F. Willemsen, J. Phys. A **16**, 3365 (1983).
[40] T. Grossman and A. Aharony, J. Phys. A **19**, L745 (1986).
[41] T. Grossman and A. Aharony, J. Phys. A **20**, L1193 (1987).
[42] R. F. Voss, J. Phys. A **17**, L373 (1984).
[43] A. Bunde and J. F. Gouyet, J. Phys. A **18**, L285 (1985).
[44] R. M. Ziff, Phys. Rev. Lett. **56**, 545 (1986).
[45] H. Saleur and B. Duplantier, Phys. Rev. Lett. **58**, 2325 (1987).
[46] S. Roux and E. Guyon, J. Phys. A **22**, 3693 (1989).
[47] L. Furuberg, K. J. Måløy and J. Feder (unpublished).

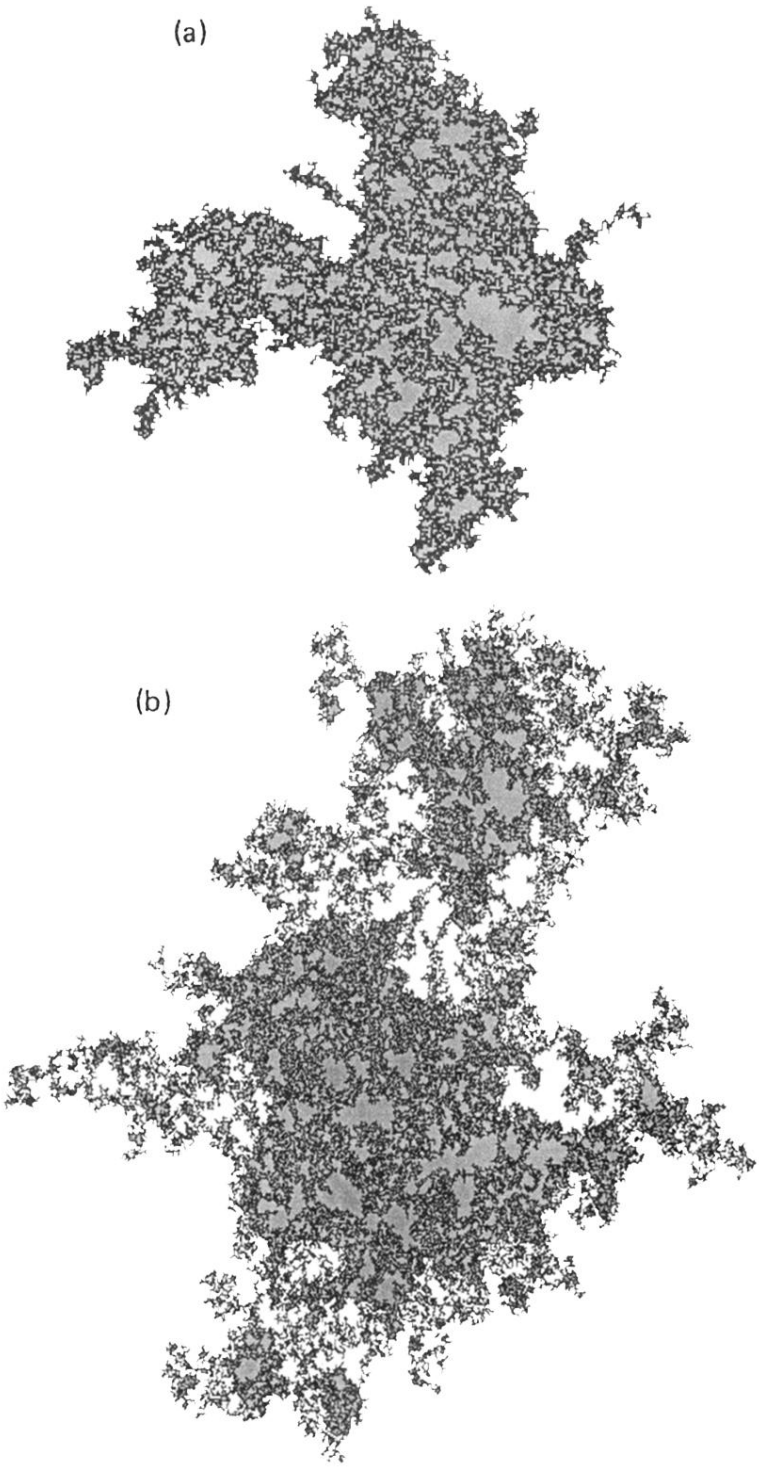

FIG. 1. Examples of two drainage areas used in the simulations. In Fig. 1(a), the boundary of the drainage area is the external perimeter of the invasion percolation cluster. The black sites are invaded sites and the gray sites are trapped sites. The maximum extension ($L = x_{max} - x_{min}$) is 256 lattice units. In Fig. 1(b), the boundary of the drainage area is the hull of an invasion percolation cluster. Those trapped areas in the cluster that can be connected to the outside through a path consisting of steps between unoccupied nearest neighbors or unoccupied next nearest neighbors are not included in the drainage area. Trapped regions that cannot be reached in this manner are shown in gray. The cluster extends over a length of 512 lattice units. In both parts of the figure, the entire drainage areas used in the simulations are indicated by the black sites and gray sites.